Regenerative Therapy 12 (2019) 20–26

Contents lists available at ScienceDirect

Regenerative Therapy

journal homepage: http://www.elsevier.com/locate/reth

Original Article

Effect of liquid flow by pipetting during medium change on deformation of hiPSC aggregates

Yuma Kato [a, 1], Takuya Matsumoto [b], Masahiro Kino-oka [a, *]

[a] Department of Biotechnology, Graduate School of Engineering, Osaka University, 2-1 Yamada-oka, Suita, Osaka, 565-0871, Japan
[b] Institute for Innovation, Ajinomoto Co., Inc., 1-1 Suzukicho, Kawasaki-ku, Kawasaki, Kanagawa, 210-8681, Japan

ARTICLE INFO

Article history:
Received 18 February 2019
Received in revised form
19 March 2019
Accepted 21 March 2019

Keywords:
Human induced pluripotent stem cells
Aggregate formation
Extracellular matrix
Fluid flow
Automation

ABSTRACT

Introduction: Maintaining the pluripotency and homogeneity of human induced pluripotent stem cells (hiPSCs) requires stable culture conditions with consistent medium change. In this study, we evaluated the performance of medium change by machine vs. medium change performed manually in terms of their impact on the aggregate shape of hiPSCs.
Methods: Aggregates of two hiPSC lines (1383D2 and Tic) were cultured, and the medium change was conducted either manually or with a machine. The populational homogeneity in aggregate shape was determined based on the projected aggregate area for size expansion as well as the circularity for spherical morphology.
Results: In the case of manually performed medium changes, the size of 1383D2 aggregates expanded homogeneously, maintaining its spherical morphology as culture duration increased, while spherical morphology was deformed in Tic aggregates, which had a heterogeneous population in terms of shape. In the case of medium change performed by a machine under a low flux of liquid flow, cultures of both aggregates showed homogeneous populations without deformation, although a high flux led to a heterogeneous population. The heterogeneous population observed in manually performed medium change was caused by the low stability of motion. In addition, time-lapse observation revealed that the Tic aggregates underwent tardive deformation with cellular protrusions from the aggregate surface after medium change with high flux. Histological analysis revealed a spatial heterogeneity of collagen type I inside 1383D2 aggregates, which had a shell structure with strong formation of collagen type I at the periphery of the aggregates, while Tic aggregates did not have a shell structure, suggesting that the shell structure prevented aggregate deformation.
Conclusion: Medium change by a machine led to a homogeneous population of aggregate shapes. Liquid flow caused tardive deformation of aggregates, but the shell structure of collagen type I in aggregates maintained its spherical shape.

1. Introduction

A reliable supply of cells is essential for cell-based therapy, drug discovery, and other applications involving human induced pluripotent stem cells (hiPSCs) [1,2]. It is assumed that cell state and number depend on the technique used by each operator when cultures are maintained manually; thus, the consistency of cultures can be negatively affected if a large number of cells is required. Automating the cell culture process can ensure the homogeneity of mass cultures. Cultured hiPSCs form aggregates and many culture protocols have been established to increase their number, while inducing their differentiation [3–5].

Cell aggregates form via cell–cell [6–8] and cell–matrix [8–10] interactions; these can be disrupted by fluid flow such as during cell collection or medium change, leading to the dissociation of cells [11]. Cells in suspension cultures are continuously agitated and

Abbreviations: hiPSCs, human induced pluripotent stem cells; ECM, extracellular matrix; hESCs, human embryonic stem cells; ROCK, Rho kinase; PBS, phosphate buffered saline.

* Corresponding author. Fax: +81 06 6879 4246.
E-mail address: kino-oka@bio.eng.osaka-u.ac.jp (M. Kino-oka).

Peer review under responsibility of the Japanese Society for Regenerative Medicine.

[1] This work is the basis for the Ph.D. dissertation of Yuma Kato.

https://doi.org/10.1016/j.reth.2019.03.004

their growth is affected by fluid flow [12]. A device that breaks up embryoid bodies by capillary flow and releases single cells has been developed [11]. However, in order to use these technologies effectively, it is important to understand the behavior of cell aggregates under conditions of mechanical stress. In one study, a rotating wall vessel was used to investigate the effect of chronic shear stress on the growth, survival, and differentiation of preimplantation embryos [13]. Although it is known that individual cells within aggregates are affected by fluid flow, changes within whole aggregates have received little attention.

The stability of cell aggregates against fluid flow varies depending on their size and structure. For example, extracellular matrix (ECM) is remodeled and synthesized on cell aggregates and covers their surface [14], preventing fluid flow from damaging the cells [15]. The ECM also affects the growth of hiPSCs in aggregates [14–16]. Furthermore, phenotypic differences caused by genetic and epigenetic variations are observed among cell lines [17,18]. Especially, Narsinh et al. [19] reported gene expression profiles of 362 hiPSCs and hESCs, and demonstrated that gene expression level in hiPSCs is more heterogeneous than that in hESCs. These variations in gene expression in hiPSCs do not only occur among individuals [20] but also donors [21]. Therefore, it is presumed that the capacity for aggregate formation and stability against fluid flow also vary among cell lines. Although several techniques have been developed to characterize cell aggregate properties [22,23], the literature on aggregate properties is limited.

The purpose of present study was to stabilize the medium change using a machine and to obtain more homogeneous shapes of aggregates than those obtained under manually performed medium change. Furthermore, we compared the stability of each aggregate formed by two different cell lines by changing the flux with regard to the medium change performed with a machine. To evaluate the stability, we compared the homogeneity of aggregate shapes and observed deformation behavior after temporal liquid flow under medium change.

2. Materials and methods

2.1. Cells and culture conditions

The hiPSC lines, 1383D2 and Tic, used in this study were obtained from the Center for iPS Cell Research and Application in Kyoto University [24] and Japanese Collection of Research Bioresources Cell Bank, respectively. The cells were maintained in ϕ100-mm dish coated with 511-laminin fragment (iMatrix-511, Nippi, Kyoto, Japan) in hiPSC culture medium (StemFit AK02N medium; Ajinomoto, Tokyo, Japan) at 37 °C in a humidified atmosphere of 5% CO_2. The maintenance cultures were conducted according to the procedure reported in our previous study [15].

2.2. Aggregate cultures

The hiPSCs were harvested from maintenance culture and dissociated into single cells as described elsewhere [16]. Viable cells were counted by the trypan blue exclusion method using a cell counter (TC20; Bio-Rad, Hercules, CA, USA). A single aggregate was cultured in a 96-well plate (ultra-low attachment V-bottom plate, Sumitomo Bakelite, Tokyo, Japan) by seeding 5.0×10^2 cells/well. The aggregate culture was conducted for 96 h. As shown in Fig. 1A, the hiPSC medium with 10 μM Rho kinase (ROCK) inhibitor (Y-27632; Fujifilm Wako Pure Chemical Corporation, Osaka, Japan) was used for the first 48 h of culture, and medium changes were conducted every 24 h after 48 h of culture time (t) using hiPSC medium without ROCK inhibitor. For medium replacement, half of the medium was replaced with a fresh medium; this was done three times either manually or by using a machine.

2.3. Quantitative analysis of hiPSC aggregate shape

In each culture, 48 aggregates ( )($n_{agg} = 48$) were prepared to analyze the shape. The projected images of hiPSC aggregates were captured using an image analysis system with a 10 × objective lens (IN Cell Analyzer 2000; GE Healthcare, Buckinghamshire, UK) to evaluate the aggregate shape. Here, the capturing was conducted before and after medium change (at $t = 48$ and 72 h) and at the end of culture (at $t = 96$ h). As shown in Fig. 1B, the aggregate shape was evaluated with the projected area of the aggregate for its expansion and circularity for its deformation from spherical morphology using image processing software (Image-Pro Plus, Media Cybernetics, Rockville, MD, USA). The image of the aggregate in 8-bit gray scale was extracted manually to convert it into a binary image for estimating the projected area of the aggregate (a) and its perimeter (l), with circularity being, $c = l^2/4\pi a$. The extent of deformation in each aggregate for certain duration (Δt) at a given culture time (t) was defined as follows:

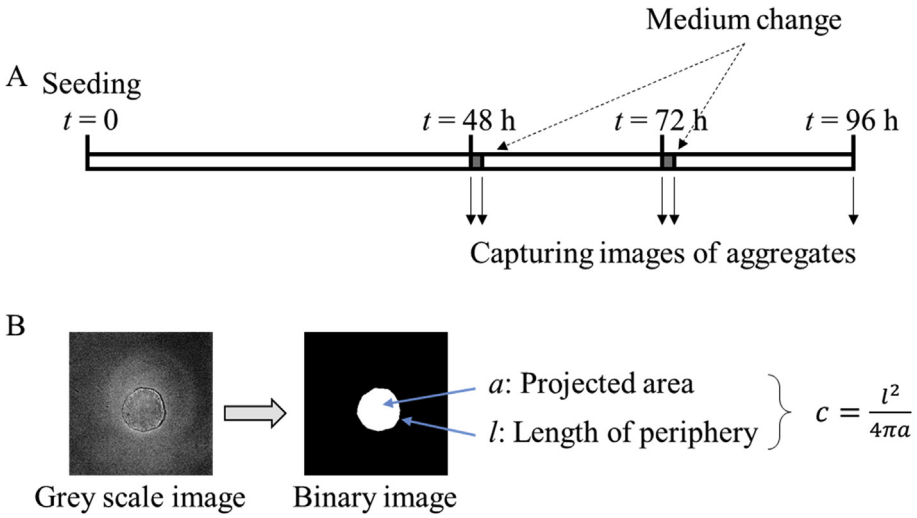

Fig. 1. Experimental procedure of aggregate culture in well. (A) Process of aggregate culture, (B) image processing of aggregates.

$$\eta_{t,\ \Delta t} = \frac{c_{t,\ \Delta t}}{c_t} \quad (1)$$

where, c_t (−) and $c_{t,\ \Delta t}$ (−) denote c before and after medium change, respectively, and t (h) and Δt (h) were set as $t = 48$ and 72 h and $\Delta t = 0$ and 24 h, respectively. The average value (η_0) and its standard error (σ) were estimated using $\eta_{t,\ \Delta t}$ at $t = 48$ h and at $\Delta t = 0$ h for 1383D2 aggregates in which medium change was performed with a machine at low flux as control. The morphological changes of aggregates under other conditions were categorized into three types; non-deformation ($\eta_{t,\ \Delta t} < \eta_0 + 10\sigma$), low deformation ($\eta_0 + 10\sigma \leq \eta_{t,\ \Delta t} < \eta_0 + 20\sigma$), and high deformation ($\eta_0 + 20\sigma \leq \eta_{t,\ \Delta t}$). The frequencies of non-deformation (f_N), low deformation (f_L), and high deformation (f_H) were obtained.

2.4. Medium change using a machine

As shown in Fig. 2, the machine for medium change (Micronix, Kyoto, Japan) consisted of a plate setting, plate cover remover, plate transfer, dispenser, and reservoirs for fresh and waste media in a laminar flow hood. The dispenser has 96 nozzles, which can change the flux of liquid flow, for withdrawing and introducing medium. In each well, the tips of the micropipettes were inserted at 1.5 mm distance from the center and 3.0 mm height from the center bottom (Fig. 2B). The inner diameter of the tip was 0.4 mm (CyBioR SELMA 96/250 μl; Analytik Jena, Jena, Germany). The flux of liquid flow at the tip was changed, and the low and high fluxes of medium flows were set to be 1.0 mm/s and 5.0×10^1 mm/s, respectively.

2.5. Time-lapse experiments

The time-lapse observation for aggregates ($n_{agg} \geq 48$) under each condition was conducted using time-lapse microscope (Biostudio imaging system, Nikon, Tokyo, Japan). The images were captured using 4 × objective lens at 5-min intervals.

2.6. Fluorescence observation for aggregate cross section

The cross sections of cell aggregates were prepared according to the procedure reported in our previous study [15]. The sections were then incubated overnight at 4 °C with primary antibody against collagen type I (Abcam, Cambridge, MA, UK) diluted in PBS with 10% Block Ace (DS Pharma Biomedical, Osaka, Japan). After washing with Tris-buffered saline and incubation in PBS containing 10% Block Ace and Alexa Fluor 594-conjugated secondary antibody (Thermo Fisher Scientific, Waltham, MA, USA) for 60 min, cell nuclei were stained with 4′,6-diamidino-2-phenylindole (Thermo Fisher Scientific, Waltham, MA, USA) for 20 min. The sections were then washed with PBS and observed with a confocal laser scanning microscope (FV-1000; Olympus, Tokyo, Japan).

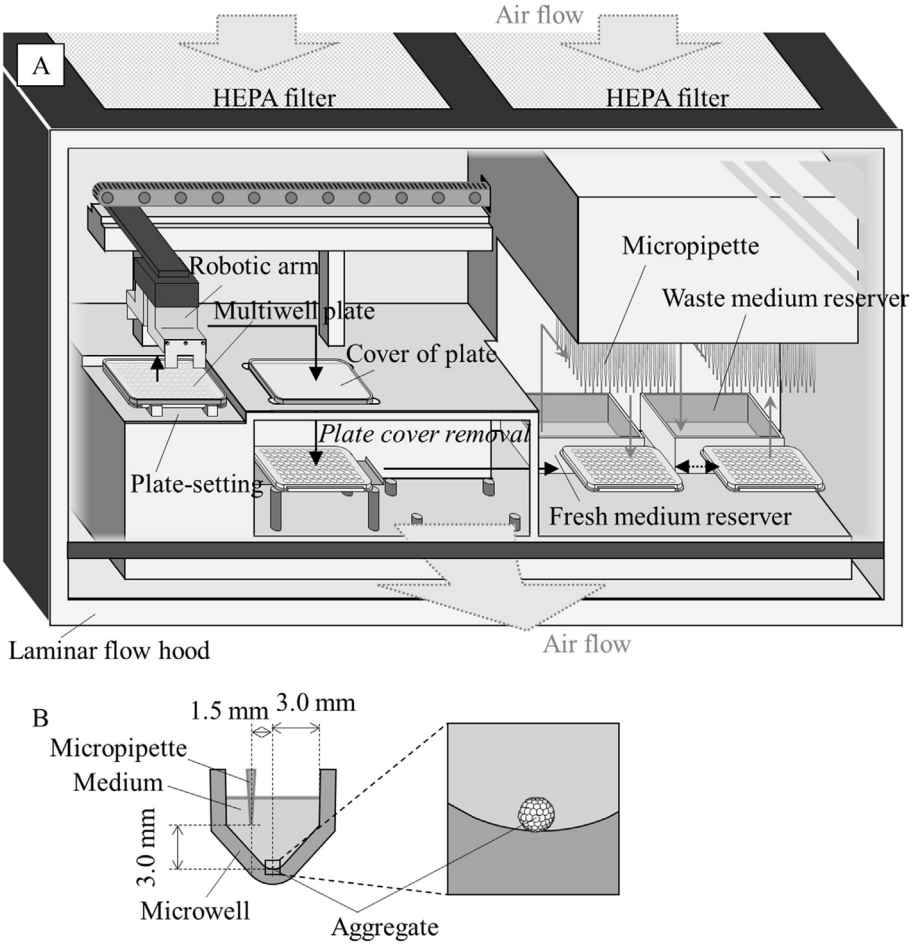

Fig. 2. Machinery medium change system for multi-well plates in the culture of hiPSC aggregates. (A) Machine for medium change. (B) Insertion position of micropipette tip in each well of the multi-well plate.

2.7. Statistical analysis

At least two independent experiments were conducted for each tested condition, and the values of circularity, c (−) and projected area, a (μm^2) were expressed as the mean ± standard error (SE) from 48 cell aggregates. To evaluate changes in c (−) and a (μm^2) based on elapsed culture time, statistical comparisons were performed using the Student's t-test and values of $P < 0.01$ were considered significant. Additionally, for change in $\eta_{t,\Delta t}$, statistical comparisons were performed in the same way.

3. Results

3.1. Aggregate shapes in cultures with medium change done manually or by a machine

The aggregates of hiPSCs were cultured for 96 h with machine or manually performed medium change at $t = 48$ and 72 h. Aggregate shapes were observed to elucidate the aggregate size and morphology using the projected area (a) and circularity (c) values, respectively. The machine for medium change was operated at 1.0 mm/s flux of liquid flow. The 1383D2 cells in the culture with manually performed medium change formed spherical aggregates at $t = 48$ h (Fig. 3a) with narrow distribution of a and c values (Fig. 3A). The average values of a and c were $\bar{a} = (5.39\pm0.08) \times 10^4$ μm^2 and $\bar{c} = 1.05\pm0.00$, respectively. As culture duration increased, a value increased with relatively wider distribution, although the c value was relatively unchanged with a narrow distribution (Fig. 3A), with the values being $\bar{a} = (1.95\pm0.03) \times 10^5$ μm^2 and $\bar{c} = 1.03\pm0.00$ at $t = 96$ h, respectively, indicating that the aggregates expanded, while maintaining their spherical morphology (Fig. 3b). In the culture in which medium change was done with a machine, similar trends in shape change were obtained ($\bar{a} = (5.44\pm0.08) \times 10^4$ μm^2 and $\bar{c} = 1.06\pm0.01$ at $t = 48$ h and $\bar{a} = (2.07\pm0.03) \times 10^5$ μm^2 and $\bar{c} = 1.04\pm0.00$ at $t = 96$ h), with expansion of the size of the spherical aggregates (Fig. 3c–d).

Similar to 1383D2 aggregates, the Tic cells in the culture with manually performed medium change formed spherical aggregates at $t = 48$ h (Fig. 3e): $\bar{a} = (5.05\pm0.07) \times 10^4$ μm^2 and $\bar{c} = 1.06\pm0.00$ (Fig. 3C). With elapsed time, c value increased with broader

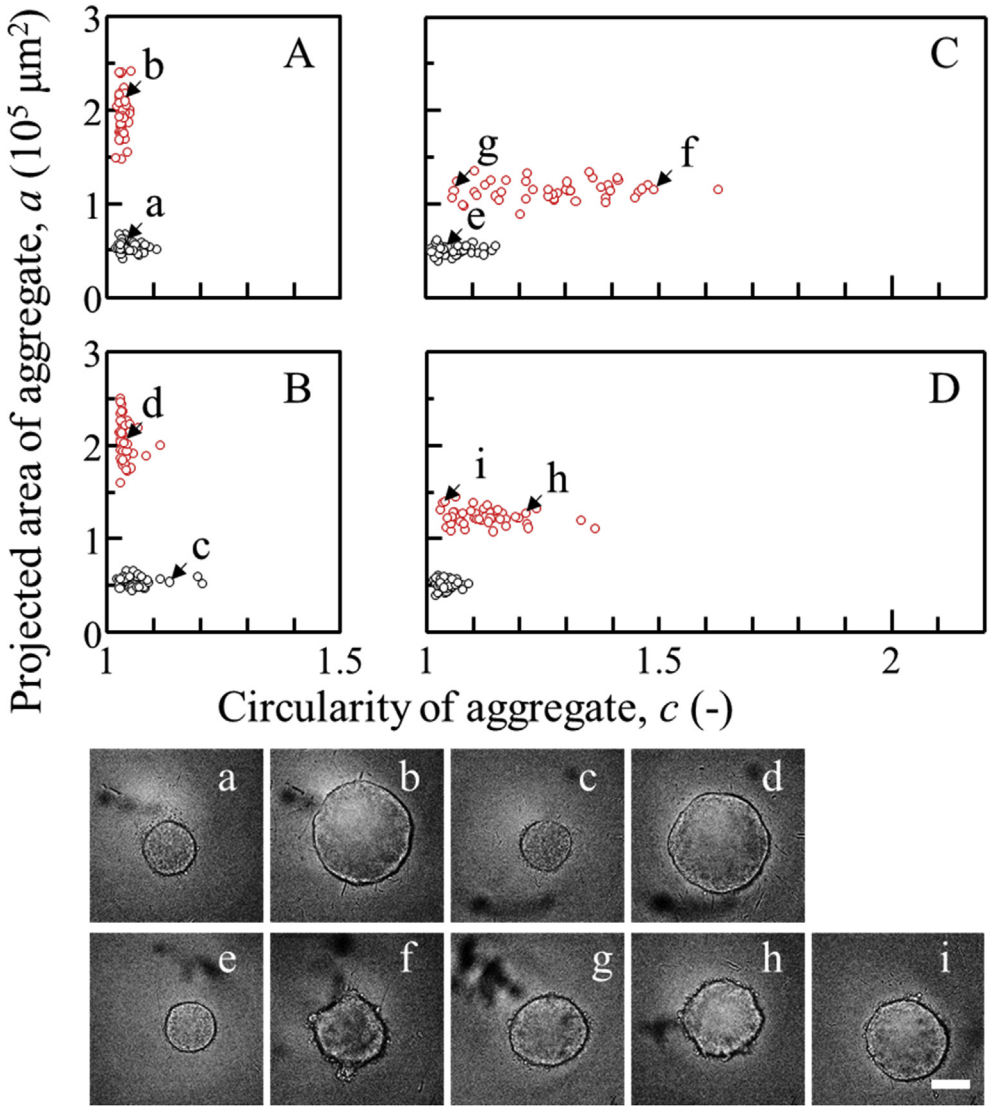

Fig. 3. Aggregate shape for expansion and morphology in the culture of 1383D2 and Tic with medium change performed manually or by a machine. (A–D) Distribution of projected area and circularity; (a–i) aggregate images in each condition. 1383D2 (A, B) and Tic (C, D) aggregates by manually (A, C) and machine (B, D)-performed medium changes. Arrows in figures show the specific aggregates. Scale bars, 200 μm. Black and red circles show the data at $t = 48$ h and 96 h, respectively.

distribution, although a value increased with a narrow distribution, with the values being $\bar{a} = (1.14\pm0.01)\times 10^5$ μm^2 and $\bar{c} = 1.28\pm0.02$ at $t = 96$ h, indicating that the spherical morphology of Tic aggregates was deformed during aggregate expansion. In addition, the Tic aggregates at $t = 96$ h exhibited protrusions on the aggregate surface (Fig. 3f), although some of the aggregates retained the spherical morphology (Fig. 3g). In the case of medium change with a machine, a reduced distribution of c was obtained at $t = 96$ h (Fig. 3D), indicating a relatively homogeneous population with spherical morphology (Fig. 3i), although some of the aggregates underwent slight deformations (Fig. 3h). These results suggest that medium change by a machine induces high motion stability, leading to populational homogeneity in aggregate shape.

3.2. Impact of fluid flow on aggregate morphology

To elucidate the impact of liquid flow upon medium change, low (1.0 mm/s) and high (5.0×10^1 mm/s) fluxes were set and the aggregate shapes were observed before and after medium change at $t = 48$ and 72 h and at the end of culture ($t = 96$ h). For 1383D2 aggregate culture, at low and high fluxes (Fig. 4A and B), the spherical aggregate morphology before and after medium change at $t = 48$ and 72 h did not change ($c \cong 1$), and the homogeneous populations in the morphology appeared at $t = 96$ h, indicating that medium change did not have any impact on aggregate morphology in 1383D2 aggregates. For Tic aggregates, at a low flux (Fig. 4C), the morphology did not change before and after medium change at $t = 48$ and 72 h, while some of the aggregates exhibited deformation with a relatively higher c value at $t = 96$ h and a broader distribution of c value at $t = 96$ h, suggesting a slow response of deformation after medium change at $t = 72$ h. In addition, the medium change at high flux (Fig. 4D) caused remarkable deformation of aggregates with a higher c value at $t = 96$ h compared with that at low flux, suggesting the tardive impact in medium change. To examine the behavior of aggregates exposed to fluid flow, we performed time-lapse imaging of representative aggregates. Most of the 1383D2 aggregates at low and high fluxes maintained their spherical morphology, although slight morphological changes at high flux were observed (Videos 1 and 2). Tic cell aggregates at low and high fluxes showed a similar behavior to 1383D2 cells up to $t = 64$ h, and protrusions appeared on the aggregate surface starting from $t = 90$ h (Videos 3 and 4).

Supplementary video related to this article can be found at https://doi.org/10.1016/j.reth.2019.03.004.

To distinguish prompt and slow responses for aggregate deformation, the transition of deformation in each aggregate was estimated to show the ratios of deformation with these classifications: non-deformation (f_N), low deformation (f_L), and high deformation (f_H) according to procedures described in section Medium change using a machine. In the case of 1383D2 aggregates at low and high fluxes (Fig. 5A and B), non-deformation occurred ($f_N \cong 1.0$) owing to the negligible ratio of low deformation (f_L) in both cases of $\Delta t = 0$ and 24 h after medium change at $t = 48$ and 72 h, indicating neither prompt ($\Delta t = 0\,h$) nor tardive ($\Delta t = 24\,h$) impact of medium change. In the case of Tic aggregates at low flux (Fig. 5C), low deformation occurred with $f_N = 0.69$ after medium change ($\Delta t = 0\,h$) at $t = 48$ h, showing a prompt impact of medium change. However, this deformation disappeared at $\Delta t = 24\,h$, with non-deformation being predominately observed ($f_N = 0.98$). After medium change at $t = 72$ h ($\Delta t = 0\,h$), the aggregates predominately exhibited non-deformation ($f_N = 0.96$), while at $\Delta t = 24\,h$, f_N value decreased to $f_N = 0.29$, changing the aggregate morphology to a low-deformation type ($f_L = 0.29$), indicating a tardive impact of medium change from $t = 72$–96 h. In the case of high flux (Fig. 5D), an immediate effect of medium change ($\Delta t = 0\,h$) at $t = 48$ h was noted with $f_L = 0.02$ and $f_H = 0.04$, and the ratio of deformation increased to $f_L = 0.25$ and $f_H = 0.27$. In addition, a second medium change at $t = 72$ h facilitated the tardive deformation with $f_L = 0.10$ and $f_H = 0.81$. These results indicated that high flux had prompt and tardive impacts for deformation of Tic aggregates, and the tardive impact at high flux appeared to be earlier and higher than that at low flux.

3.3. Collagen type I formation in cell aggregate

To estimate the distribution of ECM in aggregates, immunostaining was conducted at $t = 96$ h to observe the localization of collagen type I. Collagen type I was distributed within 1383D2 aggregates, and the band of collagen type I appeared at the periphery to cover the outer part of cells that existed on the aggregate surface (Fig. 6A). On the other hand, Tic aggregates showed a relatively low formation of collagen type I, and a weak and disconnected band existed at the aggregate periphery (Fig. 6B).

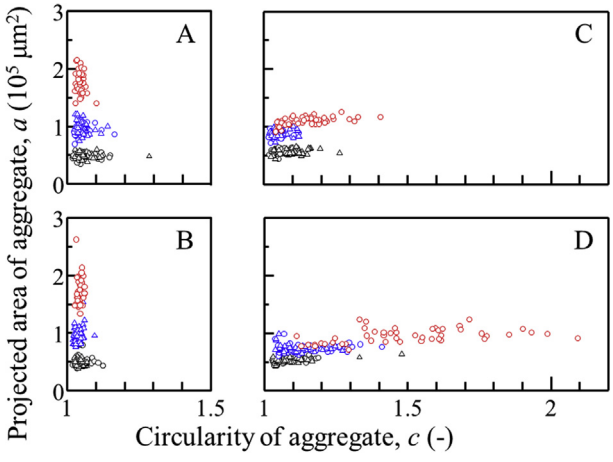

Fig. 4. Impact of liquid flow on aggregate shape in medium change by machine in culture of 1383D2 and Tic aggregates. 1383D2 (A, B) and Tic (C, D) aggregate shape at low (A, C) and high (B, D) fluxes. Symbols; circles and triangles are the data before and after medium change, respectively, at $t = 48$(black), 72 (blue), 96 h (red).

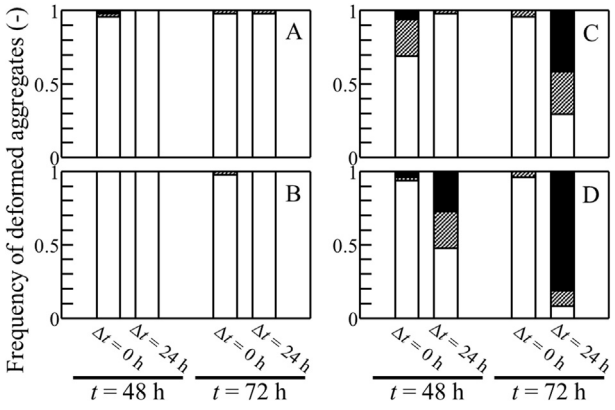

Fig. 5. Prompt and tardive changes in aggregate morphology. Ratio of deformation for 1383D2 (A, B) and Tic (C, D) aggregates at low (A, C) and high (B, D) fluxes. Symbols; open, hatched, and closed bas are the ratios of non-deformation (R_N), low deformation (R_L), and high deformation (R_H), respectively.

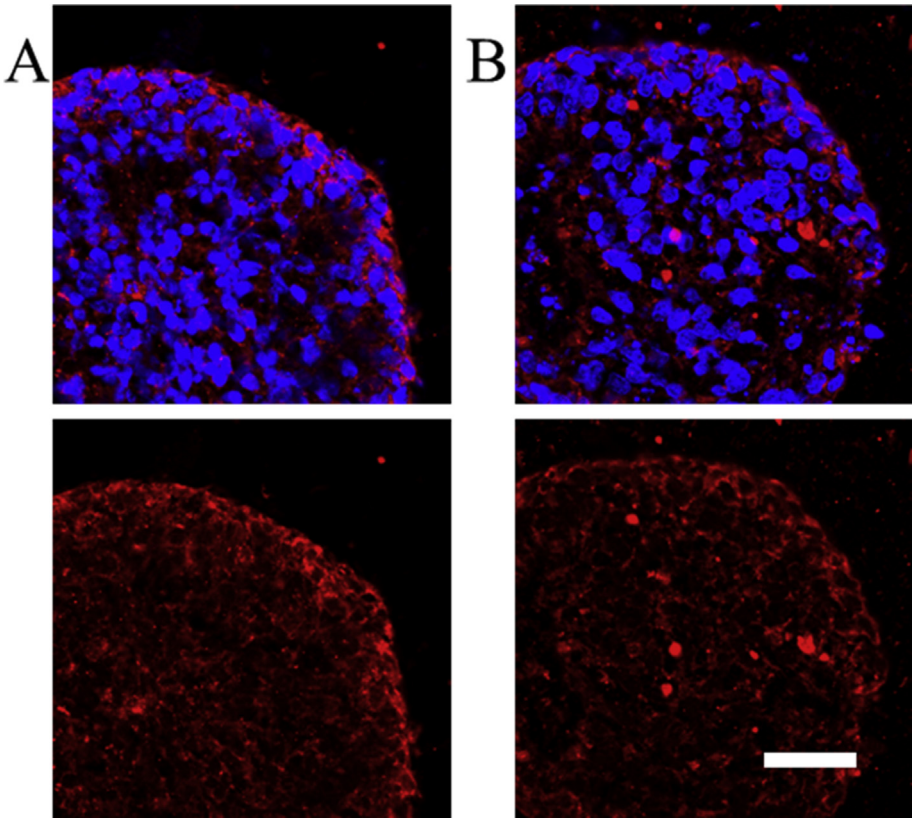

Fig. 6. Fluorescent cross-sectional images for collagen type I (red) and nucleus (blue) of 1383D2 (A) and Tic (B) aggregates. Scale bar, 50 μm.

4. Discussion

Medium change performed manually using a pipette made less accuracy to flux for addition and reduced the accuracy of medium removal as compared to medium change using a machine, as it easily induced fluctuations in medium flow to each aggregate during medium change. This impact of medium change caused different trends in aggregate morphology. Neto et al. mentioned that the precision of liquid sample preparation is improved by using the digital syringe methodology [25]. A previous study showed that the fluid flow in a microfluidic channel was higher than the set flow rate, which caused cells to detach [26]. For large-scale stem cell culture operations, it is critical to determine and be able to predict the impact of such perturbations on cell behavior [27]. A machinery system can minimize flux fluctuations, leading to a homogeneous population of aggregate shape. In this study, the variability inherent in the manual aspiration and dispensing of medium in culture wells caused a heterogeneity in aggregate shape, but only in the Tic line (Fig. 3C and D); this was improved by using a machine for the medium change process (Fig. 4C and D). These results indicate that Tic aggregates are more sensitive to fluid flow than 1383D2 aggregates and that perturbation of flux can lead to variability in aggregate morphology. Koike et al. formed cell aggregates from embryonic stem cells by seeding a different number of cells and using a different method, and found that the trend of differentiation varies based on aggregate morphology [28]. Therefore, our results suggest the improvement of differentiation efficiency by controlling the liquid flow in the culture.

Fig. 7 shows a schematic illustration, based on the current data, for differences in aggregate deformation by temporal liquid flow depending on ECM formation. ECM is deposited on the exterior of embryoid bodies during the first few days of development, forming a shell structure that prevents the diffusion of molecules [13]. We observed a similar structure around cultured 1383D2 aggregates, as evidenced by collagen type I formation at the periphery of aggregates (Fig. 6A). Our previous research showed that ECM surrounding cell aggregates prevents growth inhibition caused by liquid flow [11]. Moreover, it has been reported that the zona pellucida—a matrix surrounding the preimplantation embryo—mitigates the lethal effects of shear stress [10]. In the present work, 1383D2 cell aggregates maintained a homogeneous spherical morphology regardless of flux when medium was changed by a machine (Fig. 4A and B). In contrast, for the Tic aggregates, collagen type I was

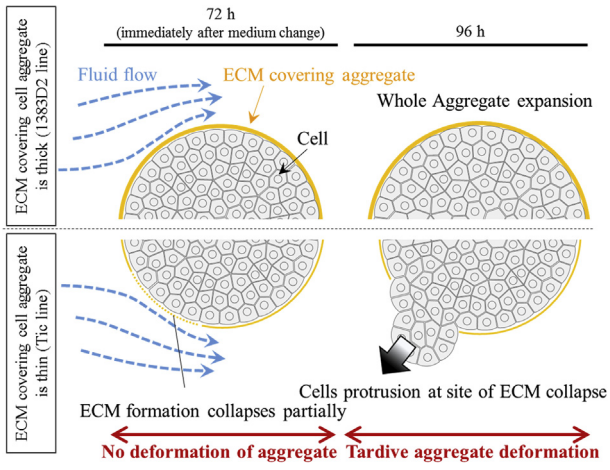

Fig. 7. Schematic illustration of the deformation mechanism for hiPSC aggregates.

detected at a low level at the periphery of aggregates (Fig. 6B); accordingly, the aggregates collapsed more readily at high flux, indicating that the aggregates were more fragile in the absence of the protective ECM and that the observed difference in aggregate morphology (i.e., deformation) between the two cell lines was due to the effects of fluid flow (Fig. 4C and D). The position of each cell in the aggregate is maintained by cell–cell adhesion [14,15]; we found that the spherical aggregates—even those formed by Tic cells—experienced little deformation as a result of fluid flow during medium change ($\Delta t = 0\ h$) (Fig. 5D), showing prompt deformation. It is possible that disruption of the ECM enables cells to migrate to the outside of aggregates, resulting in a change in aggregate morphology at $\Delta t = 24\ h$ (Fig. 5D and Video 4). This slow response of aggregates indicates tardive deformation. An ectodermal explant compressed in a parallel plate eventually relaxed into the original shape [29], and gradual deformation has been observed in cell aggregates aspirated by micropipette [30]. Additional studies are needed to clarify the relationship among changes in ECM, cell adhesion, and individual cells within hiPSC aggregates in order to fully optimize conditions for large-scale culturing.

In conclusion, this study demonstrated that medium change by a machine prevents fluctuations in morphological change as compared to manually performed medium change. The mode of medium change in culture using Tic cells caused tardive deformation of aggregate morphology, and the lower flux of liquid prevented deformation. Medium change by a machine at low flux induces a homogeneous morphology.

Acknowledgments

This work was supported by the “Development of Cell Production and Processing Systems for Commercialization of Regenerative Medicine” project, Japan Agency for Medical Research and Development, Japan. Medium change by machine was also technically supported by Micronix Inc., Japan.

Appendix A. Supplementary data

Supplementary data to this article can be found online at https://doi.org/10.1016/j.reth.2019.03.004.

References

[1] Singh VK, Kalsan M, Kumar N, Saini A, Chandra R. Induced pluripotent stem cells: applications in regenerative medicine, disease modeling, and drug discovery. Front Cell Dev Biol 2015;3:2.
[2] Shi Y, Inoue H, Wu JC, Yamanaka S. Induced pluripotent stem cell technology: a decade of progress. Nat Rev Drug Discov 2017;16(2):115–30.
[3] Sato H, Idiris A, Miwa T, Kumagai H. Microfabric vessels for embryoid body formation and rapid differentiation of pluripotent stem cells. Sci Rep 2016;6:31063.
[4] Qu Y, Han B, Gao B, Bose S, Gong Y, Wawrowsky K, et al. Differentiation of human induced pluripotent stem cells to mammary-like organoids. Stem Cell Rep 2017;8(2):205–15.
[5] Hattori N. Cerebral organoids model human brain development and microcephaly. Mov Discord 2014;29(2):185.
[6] Katsamba P, Carroll K, Ahlsena G, Bahna F, Vendome J, Posy S, et al. Linking molecular affinity and cellular specificity in cadherin-mediated adhesion. Proc Natl Acad Sci U S A 2009;106(28):11594–9.
[7] Saias L, Gomes A, Cazales M, Ducommun B, Lobjois V. Cell-cell adhesion and cytoskeleton tension oppose each other in regulating tumor cell aggregation. Cancer Res 2015;75(12):2426–33.
[8] Lin RZ, Chou LF, Chien CCM, Cheng HY. Dynamic analysis of hepatoma spheroid formation: role of E-cadherin and beta1-integrin. Cell Tissue Res 2006;324(3):411–22.
[9] Zeng D, Ou DB, Wei T, Ding L, Liu XT, Hu XL, et al. Collagen/β1 integrin interaction is required for embryoid body formation during cardiogenesis from murine induced pluripotent stem cells. BMC Cell Biol 2013;14:5.
[10] Robinson EE, Zazzali KM, Corbett SA, Foty RA. Alpha5beta1 integrin mediates strong tissue cohesion. J Cell Sci 2003;116:377–86.
[11] Papantoniou I, Hoare M, Veraitch FS. The release of single cells from embryoid bodies in a capillary flow device. Chem Eng Sci 2011;66(4):570–81.
[12] Wang Y, Chou BK, Dowey S, He CX, Gerecht S, Cheng LZ. Scalable expansion of human induced pluripotent stem cells in the defined xeno-free E8 medium under adherent and suspension culture conditions. Stem Cell Res 2013;11(3):1103–16.
[13] Xie YF, Wang FF, Zhong WJ, Puscheck E, Shen HL, Rappolee DA. Shear stress induced preimplantation embryo death that is delayed by the zona pellucida and associated with stress-activated protein kinase-mediated apoptosis. Biol Reprod 2006;75(1):45–55.
[14] Sachlos E, Auguste DT. Embryoid body morphology influences diffusive transport of inductive biochemicals: a strategy for stem cell differentiation. Biomaterials 2008;29(34):4471–80.
[15] Kato Y, Kim MH, Kino-oka M. Comparison of growth kinetics between static and dynamic cultures of human induced pluripotent stem cells. J Biosci Bioeng 2018;125(6):736–40.
[16] Nath SC, Horie M, Nagamori E, Kino-oka M. Size- and time-dependent growth properties of human induced pluripotent stem cells in the culture of single aggregate. J Biosci Bioeng 2017;124(4):469–75.
[17] Cahan P, Daley GQ. Origins and implications of pluripotent stem cell variability and heterogeneity. Nat Rev Mol Cell Biol 2013;14(6):357–68.
[18] Leha A, Moens N, Meleckyte R, Culley OJ, Gervasio MK, Kerz M, et al. A high-content platform to characterise human induced pluripotent stem cell lines. Methods 2016;96:85–96.
[19] Narshinh KH, Sun N, Sanchez-Freire V, Lee AS, Almeida P, Hu S, et al. Single cell transcriptional profiling reveals heterogeneity of human induced pluripotent stem cells. J Clin Investig 2011;121(3):1217–21.
[20] Kilpinen H, Goncalves A, Leha A, Afzal V, Alasoo K, Ashford S, et al. Common genetic variation drives molecular heterogeneity in human iPSCs. Nature 2017;546(7658):370–5.
[21] Li C, Klco JM, Helton NM, George DR, Mudd JL, Miller CA, et al. Genetic heterogeneity of induced pluripotent stem cells: results from 24 clones derived from a single C57BL/6 mouse. PLoS One 2015;10(3):e0120585.
[22] Khalifat N, Beaune G, Nagarajan U, Winnik FM, Brochard-Wyart F. Soft matter physics: tools and mechanical models for living cellular aggregates. Jap J Appl Phys 2016;55(11):1102A8.
[23] Stirbat TV, Tlili S, Houver T, Rieu JP, Barentin C, Delanoe-Ayari H. Multicellular aggregates: a model system for tissue rheology. Eur Phys J E (EPJ E) – Soft Matter 2013;36(8):84.
[24] Nakagawa M, Taniguchi Y, Senda S, Takizawa N, Ichisaka T, Asano K, et al. A novel efficient feeder-free culture system for the derivation of human induced pluripotent stem cells. Sci Rep 2014;4:3594.
[25] Neto R, Gooley A, Breadmore MC, Hilder EF, Lapierre F. Precise, accurate and user-independent blood collection system for dried blood spot sample preparation. Anal Bioanal Chem 2018;410(14):3315–23.
[26] Zhou J, Ren K, Dai W, Zhao Y, Ryan D, Wu H. Pumping-induced perturbation of flow in microfluidic channels and its implications for on-chip cell culture. Lab Chip 2011;11(13):2288–94.
[27] Kinney MA, Sargent CY, McDevitt TC. The multiparametric effects of hydrodynamic environments on stem cell culture. Tissue Eng B Rev 2011;17(4):249–62.
[28] Koike M, Sakaki S, Amano Y, Kurosawa H. Characterization of embryoid bodies of mouse embryonic stem cells formed under various culture conditions and estimation of differentiation status of such bodies. J Biosci Bioeng 2007;104(4):294–9.
[29] Schotz EM, Lanio M, Talbot JA, Manning ML. Glassy dynamics in three-dimensional embryonic tissues. J R Soc Interface 2013;10(89):20130726.
[30] Guevorkian K, Gonzalez-Rodriguez D, Carlier C, Dufour S, Brochard-Wyart F. Mechanosensitive shivering of model tissues under controlled aspiration. Proc Natl Acad Sci U S A 2011;108(33):13387–92.